

Mixing property of symmetrical polygonal billiardsR. B. do Carmo ^{1,*} and T. Araújo Lima ^{2,†}¹*Laboratório de Física, Instituto Federal de Alagoas, AL 57460-000, Brazil*²*Departamento de Física, Universidade Federal Rural de Pernambuco, Recife, PE 52171-900, Brazil*

(Received 14 August 2023; accepted 6 December 2023; published 26 January 2024)

The present work consists of a numerical study of the dynamics of irrational polygonal billiards. Our contribution reinforces the hypothesis that these systems can be strongly mixing, although never demonstrably chaotic, and discusses the role of rotational symmetries on the billiards boundaries. We introduce a biparametric polygonal billiard family with only C_n rotational symmetries. Initially, we calculate through the relative measure $r(\ell, \theta; t)$ the phase space filling. This is done for some integer values of n and for a plane of parameters $\ell \times \theta$. From the resulting phase diagram, we can identify the fully ergodic systems. The numerical evidence that symmetrical polygonal billiards can be strongly mixing is obtained by evaluating the position autocorrelation function $\text{Cor}_x(t)$, which follows a power-law-type decay $t^{-\sigma}$. The strongly mixing property is indicated by $\sigma = 1$. For odd, small values of n , the exponent $\sigma \simeq 1$ is found. On the other hand, $\sigma < 1$ (weakly mixing cases) for small, even values of n . Intermediate n values present $\sigma \simeq 1$ independently of parity. For larger values of symmetry parameter n , the biparametric family tends to be a circular billiard (integrable case). For such values of n , we identified even less ergodic behavior at the pace at which n increases and σ decreases.

DOI: [10.1103/PhysRevE.109.014224](https://doi.org/10.1103/PhysRevE.109.014224)**I. INTRODUCTION**

Ergodic theory is a branch of mathematics that classifies dynamical systems according to their degree of randomness. In ascending order: Ergodic (E), mixing (M), Kolmogorov (K), and Bernoulli (B) systems. Among them, K and B are the only ones exhibiting chaotic behavior, characterized by a positive Kolmogorov-Sinai entropy h_{KS} (or Lyapunov exponent), so that $E \supset M \supset K \supset B$ [1,2]. Mixing systems are further subclassified into weakly mixing (WM) and strongly mixing (SM) systems.

Billiards are prototype models in the ergodic theory of Hamiltonian systems. Two-dimensional billiards correspond to a particle moving in a region with reflecting walls, and the resulting dynamics can range from regular to completely chaotic depending on the billiard's shape. Over the last decades, a large number of analytical and numerical works provided results that boosted the field of nonlinear dynamics [3]. Nevertheless, some systems still benefit from further investigation. In particular, the systems related to polygonal billiards, which have $h_{KS} = 0$ and thus are not chaotic. With a few exceptions, polygonal billiards are not integrable and exhibit random behavior. Such billiards are known as pseudointegrable [4], and are characterized by a topological genus [5]. These systems can be separated into two classes: The rational polygons, where at least one internal angle is rational with π , and the irrational ones, where all internal angles are irrational with π . The class of irrational polygons has infinite genus [6].

On the dynamics of rational polygons, several mathematical results have been published over the last four decades, such as the work by Katok [7], which demonstrated that SM behavior never occurs in this particular billiard class. Years later, Kerckhoff *et al.* [8] dealt with ergodicity, while Gutkin and Katok [9] shown the WM behavior in polygons with vertical or horizontal sides. Recently, this topic was revisited by Sabogal and Troubetzkoy in Ref. [10]. One of the latest advances on rational polygons dynamics was presented in the study of Ávila and Delecroix [11], which investigated the connection between WM and regular polygonal billiards. We emphasize that for the mathematical community, polygonal billiards are never SM [12,13], although no proof of this fact has been given until now.

Regarding the understanding of irrational polygons, some works [14], particularly the one by Casati and Prosen (CP) [15], shed light on the dynamics of such polygons by providing robust numerical evidence that irrational, triangular billiards are mixing systems. Reference [16] later reinforced such CP hypothesis. To date, there is no robust study on the mixing property of nontriangular irrational billiards. Only recently, Ref. [17] has provided numerical evidence that irrational hexagons can be a mixing system, corroborating the numerical evidence from CP. More specifically, a biparametric family of irrational hexagonal billiards with the property of discrete rotational symmetry was introduced.

In classical mechanics, continuous symmetries lead to conserved quantities of the system. This result is a theorem due to the mathematician Noether [18–21]. Discrete symmetries were only studied years later. For example, in Refs. [22,23], Lutsky introduced a method for deriving conserved quantities from discrete symmetries. On the other hand, Aguirre and Krause carried out extensive studies and explicitly

*Corresponding author: ricardo.carmo@ifal.edu.br

†tiago.araujol@ufrpe.br

generalized and obtained the point symmetry group, including the covariant form [24–26]. Cicogna and Gaeta studied the presence of Lie point symmetries in dynamical systems either in Newton-Lagrange or Hamilton forms [27]. In Hamiltonian systems, properties of symmetry of the phase space come from an interplay between the symmetries of an integrable Hamiltonian and perturbations [5]. In quantum mechanics, symmetries cause states of degenerate energy [17,28–34].

In this paper, we study the classical dynamics of C_n -symmetrical polygonal billiards (C_n -SPB) that repeat themselves under a rotation of $2\pi/n$. Here, n is the symmetry parameter. Our results show that these billiards present the SM property depending on the parity of the symmetry parameter as long as n is small. Nevertheless, such dependence with the parity is missed for intermediate values of n . The impact of symmetry on ergodic properties has been discussed recently for the case of triangular billiards with symmetry under reflection about a median [35,36]. Thus, the present work also motivates the development of mathematical results of the ergodic theory of dynamical systems.

This paper is organized as follows. In Sec. II, we introduce the constraints and parameters needed to obtain the geometric shape of the C_n -SPB family. The general behavior of the phase space is also presented. Section III presents an extensive numerical calculation of the relative measure function for different parities of n . For some selected billiards, we show in Sec. IV different correlation decays, indicating WM or SM behaviors. Section V presents the impact of larger values of n on the dynamics exhibited in the C_n -SPB. For such large n values, the billiards family tends to a widely regular, circular border. Finally, concluding remarks and perspectives are presented in the last section, in addition to a comment regarding the quantization of the proposed billiards.

II. C_n -SYMMETRICAL POLYGONAL BILLIARDS AND REDUCED PHASE SPACE

The billiards family introduced in this work are convex polygons generated by alternating two adjacent sides of different lengths. One of the sides is unitary, while the other is a line segment of length $0 < \ell < 1$. In addition, θ represents the angle between these two adjacent sides (see Fig. 1). The set of adjacent sides is repeated n times depending on the desired polygonal symmetry, and the final shapes are symmetrical by rotation around the geometric center. Therefore, the billiards are C_n symmetric for $n \geq 2$, and thus, they have the same shape when rotated by an angle of $2\pi/n$. For a given billiard, the total number of segments is $2n$, and the internal alternating angles are θ and $2\pi(1 - 1/n) - \theta$. The top panels of Fig. 1 show examples of two final generic shapes generated by our building procedure: Fig. 1(a) is a C_3 -symmetric polygon, while Fig. 1(b) is C_4 symmetric. In this building procedure, the billiards become convex if the parameter θ is within the interval $\theta_n^{(\min)} < \theta < \theta_n^{(\max)}$, where $\theta_n^{(\min)} = \pi(1 - 2/n)$ and $\theta_n^{(\max)} = \pi$. Outside this interval, the polygon can be nonconvex, as shown in the bottom panels of Fig. 1. We stress that our analysis will not be carried out in this group of polygons (nonconvex). In addition, all inner angles are irrational with π , for which the numerically calculated genus is around 10^{17} [37].

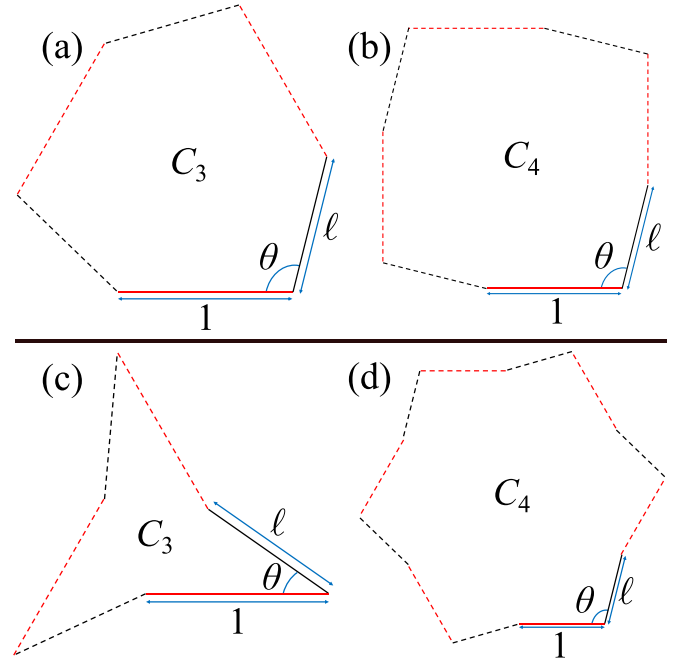


FIG. 1. Examples of symmetrical polygonal billiards (SPB) with geometric parameters (ℓ, θ) . The boundaries are formed by alternating adjacent sides of unitary and $0 < \ell < 1$ lengths. θ represents the angle between these adjacent sides. (a) SPB with symmetry C_3 . The boundary repeats itself after consecutive rotations of $2\pi/3$ or 120° (dashed lines). (b) Another example of an SPB with symmetry C_4 where the border repeats itself after consecutive rotations of $2\pi/4$ or 90° (dashed lines). (c) and (d) are nonconvex versions of the polygons depicted in (a) and (b). Our analysis will not be carried out in this group of polygons.

To illustrate a typical dynamics in the real space associated with a C_n -SPB, we depict in the left panel of Fig. 2 the representation of 200 collisions occurring in a C_5 -SPB with $(\ell, \theta) = (0.61, 2.819573\dots)$. This is done for an arbitrary initial condition. The characterization of the dynamics of such billiard is carried out from collisions in a Poincaré section, i.e., although the entire boundary is part of the dynamics, we only compute the interaction of the particle with a single line segment, being the unitary, horizontal segment the chosen one

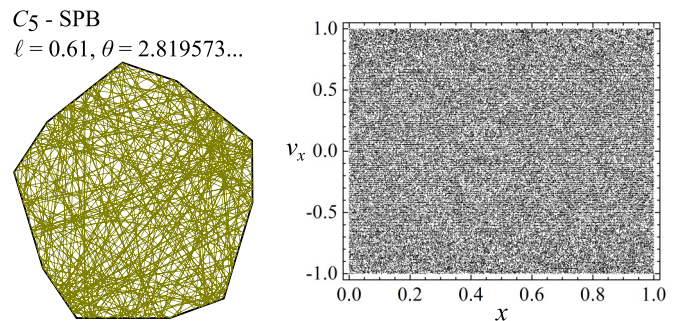


FIG. 2. Left: Typical trajectory in the real space for a C_5 -SPB after 200 collisions of the particle with the billiard's boundary. Right: Corresponding reduced phase space (x, v_x) for the C_5 -SPB shown in the left panel after 10^5 collisions with the unitary, horizontal line segment.

[15–17,33,38]. At a given discrete time t , the particle departs from the section at position x with a tangent velocity to the border denoted as v_x . A reduced phase space is then defined by the intervals $0 < x < 1$ and $-1 < v_x < 1$. In the right panel of Fig. 2, we present the reduced phase space for $t = 10^5$ collisions in the C_5 -SPB with $(\ell, \theta) = (0.61, 2.819573\dots)$, which exhibits full ergodicity. In the next section, we investigate how the phase space filling evolves with time for different values of the symmetry parameter n . Billiards with a fast tendency toward ergodicity will be candidates to be SM.

III. RELATIVE MEASURE

In this section, we investigate how fast the phase space of a given billiard is filled, focusing on the influence of its rotational symmetry on this process. More specifically, we are interested in the dependence of the phase space filling with the parity of the symmetry parameter n . We initiate our explorations by first partitioning the reduced phase space (x, v_x) into a large number N_C of cells. In our numerical calculations, we utilize $N_C = 10^6$. Then, let $m(t)$ be the number of cells visited up to collision t for a given trajectory, and $\langle m(t) \rangle$ the average for different orbits with random initial conditions. Thus, the relative measure, i.e., the average fraction of visited cells, is given by $r(t) = \langle m(t) \rangle / N_C$. As predicted by the random model (RM) [39], if all cells have the same probability of being visited, then $r(t) = r_{\text{RM}}(t)$, where

$$r_{\text{RM}}(t) = 1 - \exp(-t/N_C). \quad (1)$$

In our first analysis, we consider SPBs characterized by the pair $(\ell, \theta) = (0.94, 2.499721\dots)$ and vary the values of n . The top panel of Fig. 3 portrays the borders of the resulting billiards ordered by the parity of n . We stress that all these billiards have $(\ell, \theta) = (0.94, 2.499721\dots)$. The relative measure $r(t)$ associated with some rotational symmetries C_n is plotted against t/N_C in the bottom panel of Fig. 3. It is evident that the curves related to even values of n do not follow the result predicted by Eq. (1), which is represented by a solid black line in this graph. Recall that the first member of the symmetrical family, i.e., the C_2 -SPB, is a parallelogram with alternating sides (unitary and ℓ lengths), with inner angles θ and $2\pi - \theta$. Such a simple geometric shape leads to a phase space filled very slowly, as one can observe in Fig. 3. On the other hand, $r(t)$ curves for odd symmetries follow the predictions of the RM very closely. Therefore, for this specific pair of parameters $(\ell, \theta) = (0.94, 2.499721\dots)$, we observe a fast filling of the phase space for the odd symmetries. Nevertheless, a broader analysis over the entire range of the parameters (ℓ, θ) as a function of the parity of n still needs to be performed. This is our next goal in this section.

In order to find billiards that may be SM or WM, we must first investigate the rate of ergodicity in such systems. The closer the behavior of the numerically computed $r(t)$ is to r_{RM} [given by Eq. (1)], the greater is the chance of a given billiard displays the SM property. To map the ergodicity of a C_n -SPB family, we evaluate $r(t = N_C)$ for a large number of billiards, up to 20000 depending on the symmetry. Note that for the RM, $r_{\text{RM}}(t = N_C) = 0.632121\dots$. The results of such calculations are shown in the phase diagrams portrayed in Figs. 4 and 5, separated into odd and even symmetries, re-

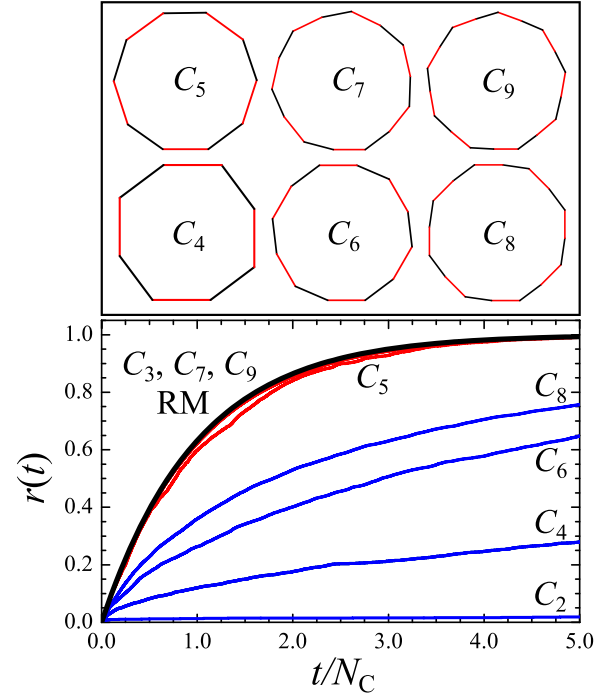


FIG. 3. Top: C_n -SPB boundaries for different values of symmetry parameter n . The geometric parameter values are $(\ell, \theta) = (0.94, 2.499721\dots)$ in all cases. Bottom: Relative measure $r(t)$ computed for some values of n . The curves associated with $n = 7, n = 9$, and with the RM [given by Eq. (1)] are almost indistinguishable. The C_2 -SPB is a simple parallelogram that does not scatter the phase space significantly.

spectively. Billiards that present $r(t = N_C)$ closer to $r_{\text{RM}}(t = N_C) = 0.632121\dots$ reach full ergodicity faster than other billiards associated with lower values of $r(t = N_C)$. Further-

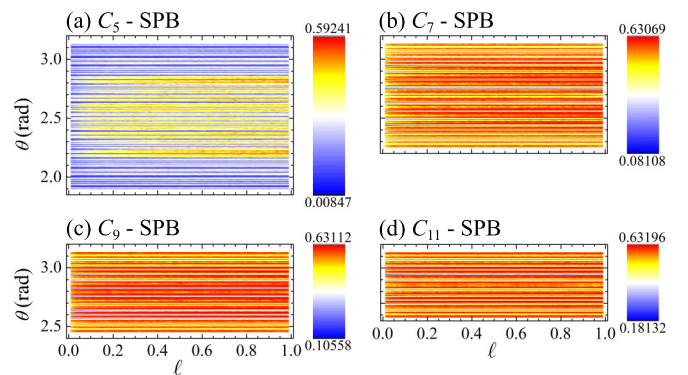


FIG. 4. Phase diagrams of $r(t = N_C)$ in the parameter space (ℓ, θ) , for odd symmetries of C_n -SPB with (a) $n = 5$, (b) $n = 7$, (c) $n = 9$, and (d) $n = 11$. Note that for the RM, $r_{\text{RM}}(t = N_C) \approx 0.63$, as evaluated by utilizing Eq. (1). For a C_5 -SPB with $(\ell, \theta) = (0.65, 2.22267\dots)$, the corresponding phase space is filled almost as the RM, resulting in $r(t = N_C) \approx 0.59$. The phase spaces associated with a C_7 -SPB with $(\ell, \theta) = (0.64, 2.471759\dots)$, a C_9 -SPB with $(\ell, \theta) = (0.93, 2.64625\dots)$, and a C_{11} -SPB with $(\ell, \theta) = (0.97, 2.71176\dots)$ are filled very similarly to the RM, with all the cases resulting in $r(t = N_C) \approx 0.63$.

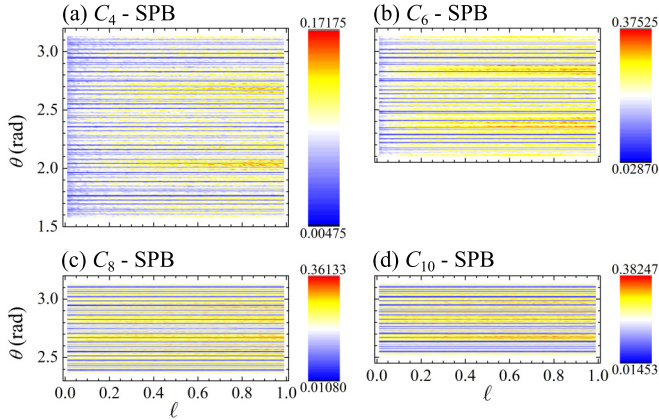


FIG. 5. Phase diagrams of $r(t = N_C)$ in the parameter space (ℓ, θ) , for even symmetries of C_n -SPB with (a) $n = 4$, (b) $n = 6$, (c) $n = 8$, and (d) $n = 10$. Note that for the RM, $r_{\text{RM}}(t = N_C) \simeq 0.63$, as evaluated by utilizing Eq. (1). A C_4 -SPB presents a scarcely filled phase space, resulting in $r(t = N_C) \simeq 0.17$ when $(\ell, \theta) = (0.88, 2.03418\dots)$. C_6 -SPB, C_8 -SPB, and C_{10} -SPB also present scarcely filled phase spaces, resulting in $r(t = N_C) \simeq 0.37$ when $(\ell, \theta) = (0.97, 2.35358\dots)$, $(\ell, \theta) = (0.99, 2.56825\dots)$, and $(\ell, \theta) = (0.8, 2.67821\dots)$, respectively. For small, even values of n , this behavior is due to the aligned parallel sides of the billiard, which does not scatter the trajectories significantly. Thus, the phase space filling is slow.

more, by comparing Figs. 4 and 5, we observe that the phase spaces for even symmetries are filled slowly. For small, even values of n , this behavior is due to the aligned parallel sides of the billiard, which does not scatter the trajectories significantly. Thus, the phase space filling is slow. On the other hand, for odd symmetries, the number of ergodic billiards is vast, highlighted in the red regions of Fig. 4. Note that the range of the parameter θ decreases as n increases, and for each phase diagram, the θ values are symmetrical with respect to the center of the range $\theta_n^{(\text{mid})} = \pi(1 - 1/n)$.

IV. DECAY OF CORRELATIONS

The characterization of the mixing dynamics of billiards is performed by utilizing the time-averaged position autocorrelation function, defined as

$$\text{Cor}_x(t) = \lim_{T \rightarrow \infty} \frac{1}{T} \sum_{\tau=0}^{T-1} x(\tau)x(\tau+t) - \langle x \rangle^2. \quad (2)$$

CP presented numerical evidence, through these functions, that the irrational triangular billiards are mixing [15]. This hypothesis was later strengthened by an extensive investigation over a wider variety of triangles and hexagons [16,17]. The classification of the mixing behavior is dictated by the power-law decay of the autocorrelation function, $|\text{Cor}_x(t)| \sim t^{-\sigma}$. When $\sigma \simeq 1$, there is numerical evidence that the system is SM.

In our next analysis, we evaluate the power-law decay of the autocorrelation function associated with some of the cases found in Figs. 4 and 5. More specifically, this dynamical behavior investigation is done for the billiards that presented the highest values of $r(t = N_C)$ shown in the phase diagrams

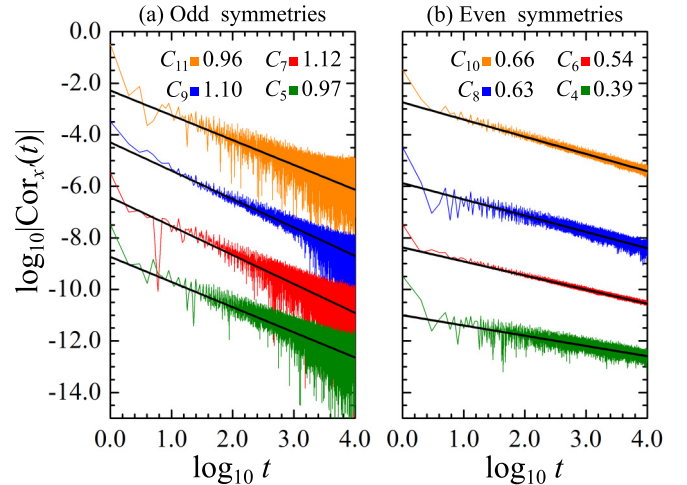


FIG. 6. Calculated position autocorrelation function $\text{Cor}_{x'}(t)$ in a decadic log-log scale for the C_n -SPB members with maximum $r(t = N_C)$ in the phase diagrams of Figs. 4 and 5. (a) Odd values of symmetry parameter n , from bottom to top, C_5 , C_7 , C_9 , and C_{11} . The decays obey power laws $|\text{Cor}_{x'}(t)| \sim t^{-\sigma}$ (represented by black lines) with exponents $\sigma \geq 0.9$, indicating SM dynamics. The specific σ values associated with each C_n are written in the plot legend. (b) Even values of n , from bottom to top, C_4 , C_6 , C_8 , and C_{10} . The decays obey power laws with exponents $\sigma < 1$, indicating the WM property. All exponents were obtained from linear fits with errors of the order of 0.001.

of Figs. 4 and 5. Such billiards can present a fast phase space filling and, consequently, are candidates to be SM. We perform the calculations in a rescaled position $x' = 2x - 1$ so that the term $\langle x' \rangle$ can be neglected in Eq. (2), since $\langle x \rangle \simeq 0.5$. All tested cases present $\langle x' \rangle \simeq 10^{-8}$.

The left panel of Fig. 6 depicts the autocorrelation functions in a decadic log-log scale corresponding to the odd symmetries C_5 – C_{11} . A tendency for fast decay of the autocorrelation functions is observed, with $\sigma \geq 0.9$ for all the cases. Here, we emphasize that the billiards with symmetries C_7 and C_9 present $\sigma \simeq 1$. Such an exponent is, therefore, numerical evidence of SM dynamics. All exponents were obtained from fits with errors of the order of 0.001. In addition, the curves have been shifted downwards for better visualization. The $\text{Cor}_{x'}(t)$ calculations for the even symmetries C_4 – C_{10} are shown in the right panel of Fig. 6. We found that $\sigma < 1$ for all the even cases, providing evidence of WM dynamics. As in the odd cases, all exponents were obtained from fits with errors around 0.001, and the curves were shifted downwards.

V. HIGHER SYMMETRIES

As we have seen during the analysis of Fig. 6, the parity of n plays a fundamental role in the dynamics of C_n -SPB. In particular, the investigations concerning odd, small values of n present the possibility of reaching SM dynamics. On the other hand, this possibility is absent for even, small values of n , being observed just WM behavior. Nevertheless, this trend is not maintained for larger values of n . When n increases, the parity becomes less and less significant, as will be clear in this section.

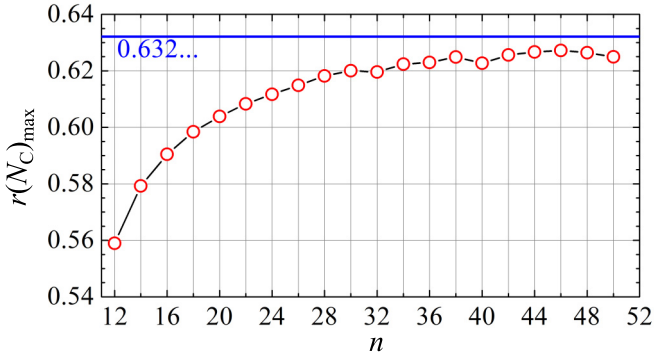


FIG. 7. Maximum value of $r(N_C)$ for even values of the symmetry parameter n . Here, we set $\ell = 0.8$. Small values of n are associated with $r(N_C)_{\max} < r_{\text{RM}}(N_C) = 0.632121\dots$, which is the expected value for the RM. As n becomes large, $r(N_C)_{\max}$ increases towards $0.632\dots$, indicating the possibility of reaching SM dynamics for billiards with these parameters.

In order to investigate the impact of larger, even values of n on the dynamics of C_n -SPB, we consider a simplified version of the phase diagram in Fig. 5. Note that $r(t = N_C)$ is approximately constant along the parameter ℓ in this phase diagram. Therefore, we set $\ell = 0.8$ and vary θ to search for the maximum value of $r(t = N_C)$. Such a process is utilized to plot the graph in Fig. 7. By inspecting this figure, we observe that as n increases, $r(N_C)_{\max}$ approaches the value $r_{\text{RM}}(t = N_C) = 0.632121\dots$, represented by the solid blue line. This enhanced phase space filling indicates the possibility of SM dynamics for billiards with these parameters. This possibility is confirmed in Fig. 8, which plots the function $\text{Cor}_x(t)$ for some of the billiards considered in Fig. 7. A tendency of fast decay of the autocorrelations is observed, with $\sigma \geq 0.9$ for all the cases. We emphasize that the billiards with symmetries C_{30} , C_{40} , and C_{50} (see the parameters in figure caption) present $\sigma \simeq 1$. All exponents were obtained from fits with errors of

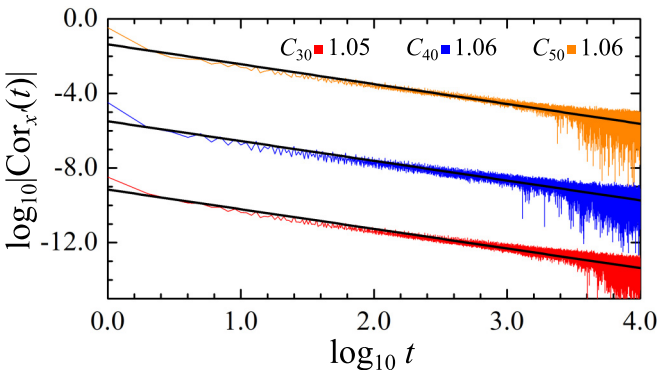


FIG. 8. Calculated position autocorrelation function $\text{Cor}_x(t)$ in decadic log-log scale for the C_n -SPB members with maximum $r(t = N_C)$ corresponding to the results of Fig. 7. From bottom to top, we show C_{30} ($\theta = 2.98634\dots$), C_{40} ($\theta = 3.0261\dots$), and C_{50} ($\theta = 3.04655\dots$), all of them with $\ell = 0.8$. The decays obey power laws $|\text{Cor}_x(t)| \sim t^{-\sigma}$ (represented by the solid black lines) with exponents $\sigma \simeq 1$, indicating SM dynamics. The specific σ values associated with each C_n are written in the plot legend. All exponents were obtained from linear fits with errors of the order of 0.001.

the order of 0.001. The curves have been shifted downwards for better visualization.

Such a change in the dynamical behavior of the C_n -SPB with even n occurs due to the increasing complexity of the polygons' boundaries as n becomes large. Recall that for small n , such as the values utilized in Secs. III and IV, the billiards are polygons with relatively few sides. The number of sides dictates how the velocities are scattered during the particle dynamics.

It is easily seen that C_n -SPB tends asymptotically to circular billiards (nonergodic) when $n \rightarrow \infty$. The resulting shape is a polygon composed of numerous sides, forming almost shallow angles between adjacent edges. As a last analysis of our work, we aim to investigate how robust the numerical approximation of the C_n -SPB dynamics is. More specifically, we are interested in checking whether the regular behavior of a circular billiard can be accessed directly from a C_n -SPB with a finite but very large value of n . To provide an answer to this question, we first need to abandon the reduced phase space idea introduced in Fig. 2. This is due to the fact that there is no flat side in circular billiards, just a point where the tangent to the curve is horizontal. Therefore, in the following, we perform our analysis in the canonical Birchoff coordinates (q, p) , where q is the perimeter fraction, and p is the tangent velocity to the border during a collision. So, $0 < q < L$, where L is the billiard perimeter and $-1 < p < 1$. In this frame, the circular billiard has an analytical map of discrete time t [13], for unitary perimeter:

$$\begin{cases} q_t = q_0 + t(\pi - 2 \arcsin p_0)/L \quad \text{mod } 1 \\ p_t = p_0. \end{cases} \quad (3)$$

The most scattered trajectory possible for this map has caustics around the circle's center.

Figure 9 shows the trajectories in the real space for two C_n -SPB: The left panel depicts the billiard for $n = 50$ and $(\ell, \theta) = (0.8, 3.04655\dots)$, while the right panel portrays the billiard for $n = 100\,000$ and $(\ell, \theta) = (0.5, 3.141561\dots)$. Both trajectories depart from the same initial conditions, i.e., $(q/L, p) = (3 \times 10^{-6}, 0.1)$. By comparing the observed trajectories for $n = 50$ and $n = 100\,000$ with the expected one for $n \rightarrow \infty$ (circular billiard), we find that the deviation is noticeable for $n = 50$. In comparison, for $n = 100\,000$ the fixed value of p deviates by merely $\sim 10^{-4}$ after 10^5 collisions. We provide a dynamical visualization of 200 collisions in the Supplemental Material [40].

Supplementing the results discussed in Fig. 9, we now present in Fig. 10 the corresponding phase spaces in Birchoff coordinates after 10^5 collisions associated with the C_{50} -SPB and C_{100000} -SPB. For $n = 50$, the graph shows a variety of accessed values, resulting in $r(N_C) \simeq 0.625$. On the other hand, for $n = 100\,000$, only a single value of p is accessed, resulting in $r(N_C) = 0.001$.

We finish our work by presenting the autocorrelation function for $n = 100\,000$ in Fig. 11. $\text{Cor}_q(t)$ decays with exponent $\sigma \simeq 0.58$, indicating that the WM behavior replaces the SM property. Note that an oscillation is expected for the regular dynamics of a circular billiard, resulting in $\sigma \simeq 0$. Therefore, we conclude that the C_n -SPB family only reproduces the regular behavior of a circular billiard for $n \rightarrow \infty$.

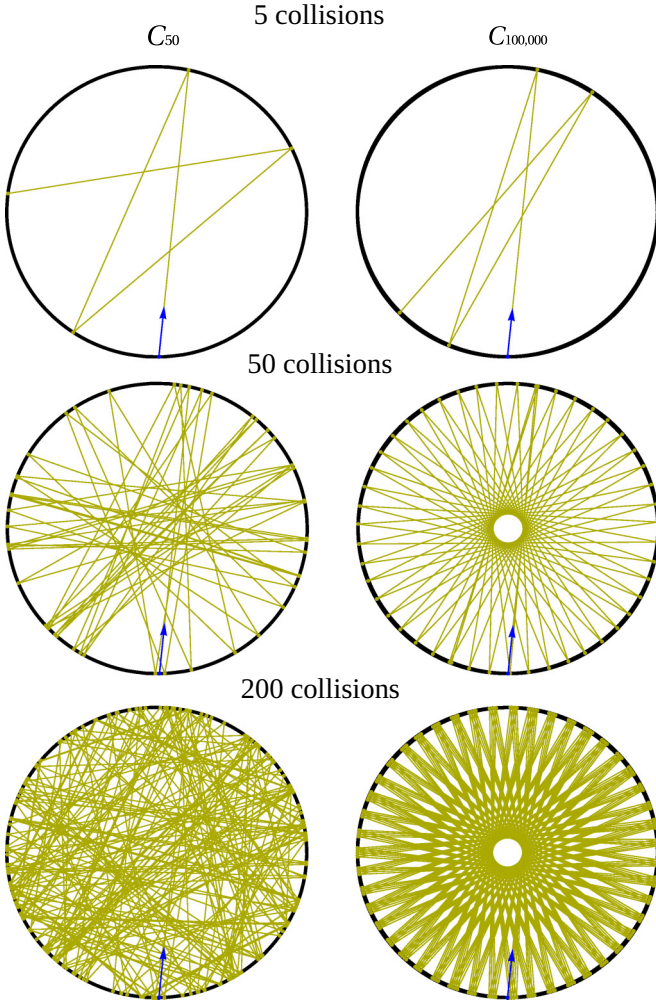


FIG. 9. Real trajectories for C_{50} with $(\theta = 3.04655\dots, \ell = 0.8)$ (on the left), and for $C_{100,000}$ with $(\theta = 3.141561\dots, \ell = 0.5)$ (on the right). The trajectories depart from the same initial condition $(q/L, p) = (3 \times 10^{-6}, 0.1)$, indicated by the arrow. Top: Real trajectory after five collisions; it is possible to identify a little deviation between the two billiards trajectories. Middle: Real trajectory after 50 collisions; the deviation between the two billiards starts to become relevant. Bottom: Real trajectory after 200 collisions; the deviation is evident now. The real trajectory is scattered for C_{50} -SPB. On the other hand, for $C_{100,000}$ -SPB, the trajectory seems regular as in a circular billiard (see Fig. 11). We provide a dynamical visualization of 200 collisions in the Supplemental Material [40].

VI. CONCLUSIONS AND PERSPECTIVES

This paper presents numerical results on the classical dynamics of symmetric irrational polygonal billiards. In our work, such billiards are convex polygons generated by alternating sides with unitary and $0 < \ell < 1$ lengths. These sides form an angle θ , and the resulting boundary is symmetric under rotations by $2\pi/n$, where n is the symmetry parameter. We investigate the possibility of finding strongly mixing dynamics in these billiards in the sense of the ergodic hierarchy of Hamiltonian systems. We start by exploring whether, for some set of geometrical parameters (ℓ, θ) and n , the corresponding dynamics tend to obey the random model (RM) [Eq. (1)]

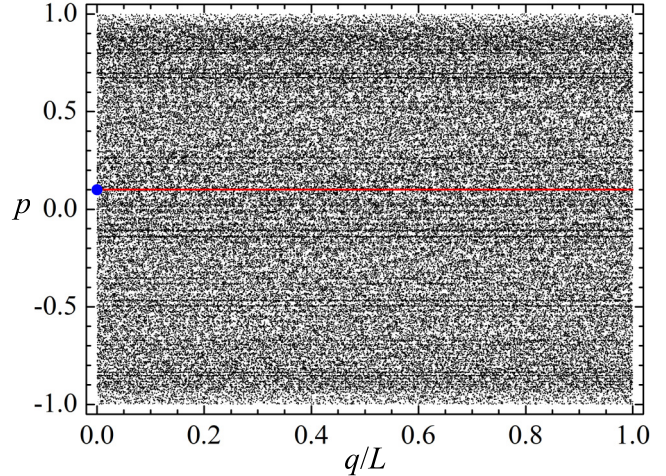


FIG. 10. Phase spaces for C_{50} -SPB (black dots) and for $C_{100,000}$ -SPB (red dots) after 10^5 collisions. In both cases, we set the initial condition as $(q/L, p) = (3 \times 10^{-6}, 0.1)$, which is represented by the blue dot. The phase space for C_{50} -SPB is scattered in agreement with its real trajectory presented in the left panel of Fig. 9). On the other hand, the phase space of the $C_{100,000}$ -SPB seems regular as in a circular billiard, with a fixed p . The deviation in p after 10^5 collisions is of the order of 10^{-4} .

[39]. We observe that for $2 \leq n \lesssim 12$, the parity of n plays a fundamental role in the behavior of the phase space. More specifically, for odd n , the most scattered dynamics found are very close to the RM (Fig. 4). On the other hand, for even n , the most scattered phase spaces are far from the RM (Fig. 5). The evidence of ergodicity is extended to the mixing property by calculating the autocorrelation functions $\text{Cor}_x(t)$ [Eq. (2)]. For selected parameters and odd symmetries, we observe a tendency for fast decaying of $\text{Cor}_x(t)$, suggesting that these billiards can exhibit strongly mixing dynamics (Fig. 6). In

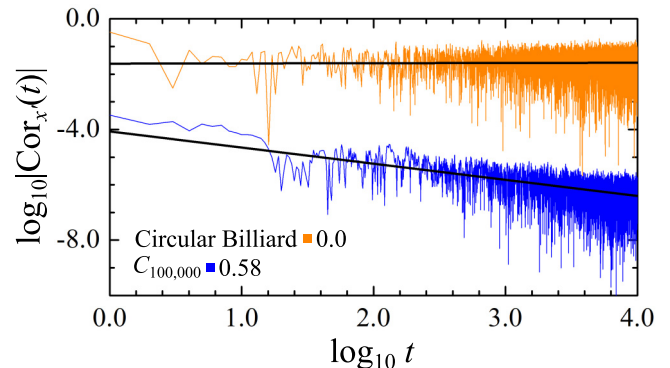


FIG. 11. Calculated position autocorrelation function $\text{Cor}_q(t)$ in decadic log-log scale for the $C_{100,000}$ -SPB and for the circular billiard (top plot). Note that the circular billiard is an integrable case and is represented by Eq. (3). The decay for $n = 100\,000$ obeys a power law $|\text{Cor}_q(t)| \sim t^{-\sigma}$ (black line) with exponent $\sigma \simeq 0.58$. On the other hand, there is no decay ($\sigma \simeq 0$) in the correlation function related to the circular billiard, which only oscillates. All exponents were obtained from linear fits with an error of around 0.01.

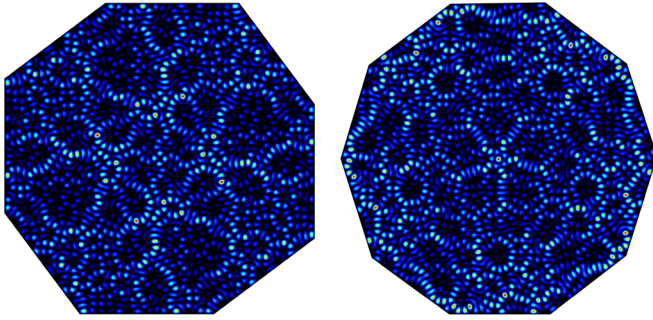


FIG. 12. Probability density $|\psi(\vec{r})|^2$ obtained numerically from the Helmholtz equation using a scaling method [46]. Small red tones indicate high probability values, while regions with dark tones indicate low values. Left: Around 2000th level for C_4 -SPB and $(\ell, \theta) = (0.94, 2.499721 \dots)$. Right: Same for C_5 -SPB.

contrast, only the weakly mixing dynamics is reached when n is even (Fig. 6).

We also find that the parity of n loses relevance for the billiard dynamics when n becomes large. When n increases, the filling of the phase spaces toward the RM also occurs for even n (Fig. 7). Thus, the strongly mixing dynamics can also be reached as long as n is sufficiently large. This effect occurs due to the increasing complexity of the billiard boundary as n increases. Recall that for small n , the billiards are polygons with relatively few sides, and the number of sides dictates how scattered the velocities are during the particle dynamics. The billiards considered in our work tends asymptotically to circular billiards (nonergodic) when $n \rightarrow \infty$. Figures 9 and 10 show how sensitive the dynamics are to the polygonal boundaries. We find that the strongly mixing property is lost for $n \gg 1$. Furthermore, the autocorrelation functions decay with exponent $\sigma < 1$, suggesting weakly mixing dynamics

(Fig. 11). We conclude that the C_n -symmetrical polygonal billiards (SPB) family only assumes the regular behavior of a circular billiard ($\sigma = 0$) when $n \rightarrow \infty$.

As a perspective for future work, quantizing the C_n -SPB is a worthy investigation. The quantum properties of pseudointegrable systems have been studied over the past decades [4,41]. However, irrational billiards have yet to be investigated [16,17,30,42]. Considering that the discrete rotational symmetries in quantized billiards produce independent spectra of singlets and doublets (degenerate states) [28,31], it should be explored how the spectral statistics are affected in the C_n -SPB, and how they are related to their classical counterparts (from WM to SM). The case of $n = 3$ was explored in irrational hexagons [17], and their spectra were analyzed with intermediate formulas between Poisson and random matrices theory statistics [43,44]. Such formulas should be tested for $n > 3$. Furthermore, the superposition of independent spectra could be studied as proposed by Ref. [45]. The eigenfunctions associated with the singlet states are symmetrical with respect to the center of the billiards, as Fig. 12 shows the probability density $|\psi(\vec{r})|^2$ of billiards with C_4 and C_5 symmetries. They were obtained by solving the Helmholtz equation, $\nabla^2 \psi_i(\vec{r}) = -k_i^2 \psi_i(\vec{r})$, with Dirichlet boundary conditions using a scaling method [46], where k_i^2 is an energy eigenvalue. Aspects related to the intensity distribution of the eigenfunctions associated with singlets and doublets must be studied in depth [47,48].

ACKNOWLEDGMENTS

Valuable discussions with F. M. de Aguiar are gratefully acknowledged. We thank P. H. A. Anjos for reading the manuscript. We are also grateful for the computational resources of LaSCoU and LCR from the Department of Physics at Universidade Federal Rural de Pernambuco.

- [1] A. M. Ozorio de Almeida, *Hamiltonian Systems: Chaos and Quantization*, 1st ed. (Cambridge University Press, Cambridge, UK, 1988)
- [2] E. Ott, *Chaos in Dynamical Systems*, 2nd ed. (Cambridge University Press, Cambridge, UK, 2002).
- [3] S. H. Strogatz, *Nonlinear Dynamics and Chaos: With Applications to Physics, Biology, Chemistry, and Engineering* (CRC Press, Boca Raton, 2018).
- [4] P. J. Richens and M. V. Berry, Pseudointegrable systems in classical and quantum mechanics, *Physica D* **2**, 495 (1981).
- [5] G. M. Zaslavsky, *The Physics of Chaos in Hamiltonian Systems*, 2nd ed. (Imperial College Press, London, 2007).
- [6] F. Valdez, Infinite genus surfaces and irrational polygonal billiards, *Geometriae Dedicata* **143**, 143 (2009).
- [7] A. Katok, Interval exchange transformations and some special flows are not mixing, *Isr. J. Math.* **35**, 301 (1980).
- [8] S. Kerckhoff, H. Masur, and J. Smillie, Ergodicity of billiard flows and quadratic differentials, *Ann. Math.* **124**, 293 (1986).
- [9] E. Gutkin and A. Katok, Weakly mixing billiards, *Holomorph. Dyn.*, 163 (1988).
- [10] A. M. Sabogal and S. Troubetzkoy, Weakly mixing polygonal billiards, *Bull. Lond. Math. Soc.* **49**, 141 (2017).
- [11] A. Avila and V. Delecroix, Weak mixing directions in non-arithmetic Veech surfaces, *J. Am. Math. Soc.* **29**, 1167 (2016).
- [12] E. Gutkin, Billiards in polygons: Survey of recent results, *J. Stat. Phys.* **83**, 7 (1996).
- [13] N. Chernov and R. Markarian, *Chaotic Billiards*, 1st ed. (American Mathematical Society, Providence, USA, 2006).
- [14] R. Artuso, G. Casati, and I. Guarneri, Numerical study on ergodic properties of triangular billiards, *Phys. Rev. E* **55**, 6384 (1997).
- [15] G. Casati and T. Prosen, Mixing property of triangular billiards, *Phys. Rev. Lett.* **83**, 4729 (1999).
- [16] T. Araújo Lima, S. Rodríguez-Pérez, and F. M. de Aguiar, Ergodicity and quantum correlations in irrational triangular billiards, *Phys. Rev. E* **87**, 062902 (2013).
- [17] T. A. Lima, R. B. do Carmo, K. Terto, and F. M. de Aguiar, Time-reversal-invariant hexagonal billiards with a point symmetry, *Phys. Rev. E* **104**, 064211 (2021).

- [18] E. Noether, Invariante Variationsprobleme, Nachrichten von der Königlichen, *Gesellschaft der Wissenschaften zu Göttingen* **1918**, 235 (1918).
- [19] J. V. José and E. J. Saletan, *Classical Dynamics. A Contemporary Approach*, 1st ed. (Cambridge University Press, Cambridge, UK, 1998).
- [20] N. A. Lemos, *Mecânica Analítica*, 2nd ed. (Ed. Livraria da Física, Sao Paulo, 2013).
- [21] N. A. Lemos, Symmetries, Noether's theorem and inequivalent Lagrangians applied to non-conservative systems, *Revista Mexicana de Física* **39**, 304 (1992).
- [22] M. Lutsky, Origin of non-Noether invariants, *Phys. Lett. A* **75**, 8 (1979).
- [23] M. Lutsky, Conservation laws and discrete symmetries in classical mechanics, *J. Math. Phys.* **22**, 1626 (1981).
- [24] M. Aguirre and J. Krause, General transformation theory of Lagrangian mechanics and the lagrange group, *Int. J. Theor. Phys.* **30**, 495 (1991).
- [25] M. Aguirre and J. Krause, Point symmetry group of the Lagrangian, *Int. J. Theor. Phys.* **30**, 1461 (1991).
- [26] J. Krause, Some remarks on the generalized Noether theory of point symmetry transformations of the lagrangian, *J. Phys. A: Math. Gen.* **25**, 991 (1992).
- [27] G. Cicogna and G. Gaeta, On Lie point symmetries in mechanics, *Il Nuovo Cimento* **107**, 1085 (1992).
- [28] F. Leyvraz, C. Schmit, and T. Seligman, Anomalous spectral statistics in a symmetrical billiard, *J. Phys. A: Math. Gen.* **29**, L575 (1996).
- [29] B. Dietz, A. Heine, V. Heuveline, and A. Richter, Test of a numerical approach to the quantization of billiards, *Phys. Rev. E* **71**, 026703 (2005).
- [30] D. D. de Menezes, M. Jar e Silva, and F. M. de Aguiar, Numerical experiments on quantum chaotic billiards, *Chaos* **17**, 023116 (2007).
- [31] Z.-Y. Li and L. Huang, Quantization and interference of a quantum billiard with fourfold rotational symmetry, *Phys. Rev. E* **101**, 062201 (2020).
- [32] B. Dietz, Relativistic quantum billiards with threefold rotational symmetry: Exact, symmetry-projected solutions for equilateral neutrino billiard, *Acta Phys. Pol. A* **140**, 473 (2021).
- [33] T. Araújo Lima and R. B. do Carmo, Classical and quantum elliptical billiards: Mixed phase space and short-range correlations in singlets and doublets, *Phys. D Nonlinear Phenomena* **458**, 134018 (2024).
- [34] W. Zhang, X. Zhang, J. Che, M. Miski-Oglu, and B. Dietz, Properties of eigenmodes and quantum-chaotic scattering in a superconducting microwave Dirac billiard with threefold rotational symmetry, *Phys. Rev. B* **107**, 144308 (2023).
- [35] K. Zahradova, J. Slipantschuk, O. F. Bandtlow, and W. Just, Impact of symmetry on ergodic properties of triangular billiards, *Phys. Rev. E* **105**, L012201 (2022).
- [36] K. Zahradova, J. Slipantschuk, O. F. Bandtlow, and W. Just, Anomalous dynamics in symmetric triangular irrational billiards, *Physica D* **445**, 133619 (2023).
- [37] S. Russ, Energy fluctuations of pseudointegrable systems with growing surface roughness, *Phys. Rev. E* **64**, 056240 (2001).
- [38] T. Araújo Lima and F. M. de Aguiar, Classical billiards and quantum fluids, *Phys. Rev. E* **91**, 012923 (2015).
- [39] M. Robnik, J. Dobnikar, A. Rapisarda, and T. Prosen, New universal aspects of diffusion in strongly chaotic systems, *J. Phys. A: Math. Gen.* **30**, L803 (1997).
- [40] See Supplemental Material at <http://link.aps.org/supplemental/10.1103/PhysRevE.109.014224> for a dynamical visualization of 200 collisions in the real space for two C_n -SPB, $n = 50$ and $n = 100\,000$. The deviation with the expected for a circular billiard is noticeable for $n = 50$ in comparison with $n = 100\,000$.
- [41] R. L. Liboff, The polygon quantum-billiard problem, *J. Math. Phys.* **35**, 596 (1994).
- [42] A. Shudo and Y. Shimizu, Extensive numerical study of spectral statistics for rational and irrational polygonal billiards, *Phys. Rev. E* **47**, 54 (1993).
- [43] M. L. Mehta, *Random Matrices*, 1st ed. (Elsevier, Amsterdam, 2004).
- [44] H.-J. Stöckmann, *Quantum Chaos: An Introduction*, 1st ed. (Cambridge University Press, Cambridge, UK, 1999).
- [45] A. Y. Abul-Magd, Level statistics for nearly integrable systems, *Phys. Rev. E* **80**, 017201 (2009).
- [46] E. Vergini and M. Saraceno, Calculation by scaling of highly excited states billiards, *Phys. Rev. E* **52**, 2204 (1995).
- [47] K. Müller, B. Mehlig, F. Milde, and M. Schreiber, Statistics of wave functions in disordered and in classically chaotic systems, *Phys. Rev. Lett.* **78**, 215 (1997).
- [48] J. Marklof and Z. Rudnick, Almost all eigenfunctions of a rational polygon are uniformly distributed, *J. Spect. Theor.* **2**, 107 (2012).